Acta Mech 197, 43–62 (2008)
DOI 10.1007/s00707-007-0503-3
Printed in The Netherlands

Acta Mechanica

On the uniqueness of solutions for the Dirichlet boundary value problem of linear elastostatics in the circular domain

A. Rohe, F. Molenkamp, W. T. Van Horssen

Delft University of Technology, Delft, The Netherlands

Received 2 April 2007; Accepted 20 August 2007; Published online 30 October 2007

Summary. The uniqueness and mathematical stability of the Dirichlet boundary value problem of linear elastostatics is studied. The problem is posed as a set of partial differential equations in terms of displacements and Dirichlet-type of boundary conditions (displacements) for arbitrary bounded domains. Then for the circular interior domain the closed form analytical solution is obtained, using an extended version of the method of separation of variables. This method with corresponding complete solution allows for the derivation of a necessary and sufficient condition for uniqueness. The results are compared with existing energy and uniqueness criteria. A parametric study of the elastic characteristics is performed to investigate the behaviour of the displacement field and the strain energy distribution, and to examine the mathematical stability of the solution. It is found that the solution for the circular element with hourglass-like boundary conditions will be unique for all $v \neq 0.5, 0.75, 1.0$ and will be mathematically stable for all $v \neq 0.75$. Locking of the circular element occurs for $v = 0.75$ as the energy tends to infinity.

List of symbols

$a_i^{(n)}$, $b_i^{(n)}$, $c_i^{(n)}$, $d_i^{(n)}$	general integration coefficients
A_{ik}	acoustic tensor, $A_{ik} = n_j\, D_{ijkl}\, n_l$
$\boldsymbol{d}_i^{(n)}$	eigenvectors of system of PDEs, Eq. (30)
D_{ijkl}	material tangent stiffness tensor
$\boldsymbol{e}_i$	unit vectors ($i = 1, 2, 3$)
e	magnitude of the prescribed enforced nodal displacement
f_r, f_θ	functions for separation of variables depending only on radius r
g_{ii}	metric coefficients ($i = 1, 2, 3$), Eq. (10)
g_r, g_θ	functions for separation of variables depending only on polar angle θ
G	shear modulus
h	auxiliary function, $h^2 = g_{11} = g_{22}$ for circular cylindrical coordinate system
H	coordinate system coefficients, Eq. (11)
$\boldsymbol{I}$	identity tensor, $\boldsymbol{I} = \delta_{ij}\boldsymbol{e}_i \otimes \boldsymbol{e}_j$
$I_i^{(n)}$	integration constants, Eq. (35)
n_i	normal vector components on the discontinuity in the velocity gradient
$r, \tilde{r}$	radius and dimensionless radius, $\tilde{r} = r/R$
$\boldsymbol{u}$	displacement vector
(x_1, x_2, x_3)	Cartesian coordinates

Correspondence: Frans Molenkamp, Geo-engineering Section, Faculty of Civil Engineering and Geosciences, Delft University of Technology, Stevinweg 1, 2628CN Delft, The Netherlands
e-mail: frans.molenkamp@citg.tudelft.nl

(r, θ, z)	polar coordinates
$\hat{v}_k$	amplitude of localising velocity
W, W_{iso}, W_{dev}	total strain energy, strain energy due to isotropic deformation, strain energy due to deviatoric deformation

Greek letters

$\boldsymbol{\varepsilon}$	(small) linear strain tensor
$\dot{\varepsilon}_{ij}$	strain increment
η, μ	separation constants
$\lambda_i^{(n)}$	eigenvalues of the system of PDEs, Eq. (29)
ν	Poisson's ratio
ξ_i	general curvilinear coordinates ($i = 1, 2, 3$) in Euclidean 3-space
$\boldsymbol{\sigma}$	Cauchy-stress tensor
$\dot{\sigma}_{ij}$	stress increment
$\varphi_r, \varphi_\theta$	radial and tangential displacement boundary conditions
$\omega^{(n)}$	auxiliary constant, Eq. (31)

Subscripts

i, j, k, l	summation indices
r	referring to radial direction
θ	referring to tangential direction

Other symbols

∇	differential operator, $\nabla = \partial \boldsymbol{e}_i / \partial x_i$
$\otimes$	dyadic or outer tensor product
$\cdot$	dot or inner tensor product
$\times$	curl
tr	trace of a vector/tensor

1 Introduction

Yet, unexplained problems occur in finite element calculations of geomechanical problems. These include numerical instabilities and non-convergence for frictional elasto-plastic material models with large dilation angles, as indicated by for example Vermeer [1], De Borst [2] or Van der Veen [3]. To begin to understand these numerical artefacts, Sellmeijer [4], Lewis [5], and Molenkamp [6] investigated the uniqueness and mathematical stability of a four-node plane finite element as a displacement-type of boundary value problem for the simplified case of an equivalent elastic material. By applying a numerical solution procedure for the so-called hourglass deformation mode with non-uniform stress and strain fields no converging solutions were found in the approximate parameter range of Poisson's ratio $0.6 < \nu < 0.9$. Furthermore, at both parameter limits locking of the element mesh was reported due to the stresses at the corners becoming infinite. These results were received with some reservations amongst others concerning the quality of the numerical solution procedure, although Molenkamp [7] obtained the same results by considering the element composed of small elements with the same properties (self-similar fractal).

To arrive at a generally convincing answer on the uniqueness and mathematical stability of a displacement-type of boundary value problem, in this paper the relatively simple problem of a circular element subjected to an hourglass-like boundary displacement is solved completely analytically. Preferably for the simulation of dilative material behaviour in the analysis a realistic elasto-plastic model should be used. However, such an analytical approach seems quite formidable. Therefore, in this paper, for simplicity, the simplest possible linear comparison solid, namely equivalent isotropic linear elasticity, is applied in a first attempt to clarify the underlying phenomena. Molenkamp [6] showed, that in order to represent the major aspects of dilative material behaviour the equivalent Poisson's ratio ν must take a larger range of values than normally considered in classical linear elasticity, namely larger than 0.5. As a result for a standard drained triaxial compression test on dense sand volume dilation can occur for increasing applied pressure.

In this study, first the existing uniqueness and stability criteria are briefly reviewed, in order to compare them with the uniqueness criterion derived for the circular interior domain here. Then, for isotropic linear elastic material behaviour the equilibrium equations based on the conservation of linear momentum are derived for a continuum. They are elaborated for a 2-dimensional cylindrical coordinate system, assuming plane strain conditions and using polar coordinates for the circular domain. The general closed form analytical solution is then obtained using an extended version of the method of separation of variables developed by Van Horssen [8], [9]. The uniqueness criterion is derived for the Dirichlet-type of boundary conditions. For hourglass-like boundary conditions the resulting displacement, strain and stress fields are elaborated. Using this complete solution its mathematical stability is examined in a parametrical study for the elastic parameter, Poisson's ratio ν.

The main difference between this work and the earlier ones [4]–[6] is that here a completely analytical solution procedure has been developed and applied, enabling the uniqueness criterion to be necessary and being based on the complete general solution of the underlying basic boundary value problem.

2 Existing uniqueness and stability criteria

The properties of materials, concerning local criteria of uniqueness and stability on the one hand and concerning the well-posedness of boundary value problems on the other, have been considered extensively during the past 150 years. The first approach was by Kirchhoff [10], [11] who derived a sufficient energy criterion, applied to an elastic material within a bounded 3-dimensional domain. Later, Cosserat [12] gave a condition for uniqueness of the solution for an ellipsoidal elastic solid. The next steps in describing the properties of the solution of the elastic problem were done by Ericksen [13], [14] with a mathematical approach, Gurtin [15] and Bramble [16] with a mechanical approach and Hill [17]–[19] investigating material stability including localisation. Recent work on localisation and failure is done by, e.g., Vardoulakis [20] or Chambon [21].

2.1 Local uniqueness criterion by Kirchhoff

The classical result of the uniqueness question is due to Kirchhoff [10], [11]. He considered 3-dimensional regions of homogeneous isotropic linear elastic materials. Modified for the plane strain situation, he proved that at most one solution exists if shear modulus G and Poisson's ratio ν obey at least the inequalities

$$G > 0 \quad \text{and} \quad -\infty < \nu < 0.5. \tag{1}$$

Equation (1) is sufficient to guarantee uniqueness. These inequalities correspond to the criterion providing positive generated energy.

2.2 Local material stability and positive-definiteness

Closely associated with the concept of uniqueness is that of material stability. Stable material behaviour is locally defined as the positiveness of the product of the stress increment $\dot{\sigma}_{ij}$ and the total strain increment $\dot{\varepsilon}_{ij}$ [18],

$$\dot{\sigma}_{ij}\dot{\varepsilon}_{ij} \geq 0, \tag{2}$$

known as Hill's condition for material stability, where the equal sign marks the onset of instability. For uniaxial loading and deformation, Eq. (2) becomes negative when the slope of the stress-strain curve is negative, the so-called strain softening regime. For incrementally linear stress-strain relations for which $\dot{\sigma}_{ij} = D_{ijkl}\dot{\varepsilon}_{kl}$, involving the material tangent stiffness tensor D_{ijkl}, Eq. (2) can be reformulated as

$$\dot{\varepsilon}_{ij}D_{ijkl}\dot{\varepsilon}_{kl} \geq 0. \tag{3}$$

Material instability therefore can occur only if at least one of the eigenvalues of D_{ijkl} is negative. Mathematically, this is associated with loss of positive-definiteness of the material tangent stiffness tensor. In case of plane strain isotropic linear elasticity positive-definiteness and therefore material stability is sufficiently guaranteed for

$$G > 0 \quad \text{and} \quad -\infty < \nu < 0.5. \tag{4}$$

For the plane strain situation of isotropic linear elasticity the local material stability criterion due to Hill (4) is equal to Kirchhoff's uniqueness and energy criterion (1).

2.3 Local criterion for localisation of deformation and ellipticity

A second local condition limiting the uniqueness of material behaviour concerns the possibility of a discontinuity surface that does not travel relatively to the material, i.e., a plane standing wave (discontinuity in the velocity gradient or localisation of deformation) [22]. For incrementally linear stress-strain relations for which $\dot{\sigma}_{ij} = D_{ijkl}\dot{\varepsilon}_{kl}$, the local stability condition reads

$$D_{ijkl}n_j n_l \hat{v}_k = 0, \tag{5}$$

in which n_i are the normal vector components on the discontinuity and $\hat{v}_k$ are the vector components of the localising velocity. The analysis then reduces to an eigenvalue problem concerning the acoustic tensor $A_{ik} = n_j\, D_{ijkl}\, n_l$. Eigenvectors $\hat{v}_k$ that generate a discontinuity in the velocity field can occur only if the determinant of the acoustic tensor vanishes. Thus the condition for instability then reads

$$\det\left(n_j D_{ijkl} n_l\right) = 0. \tag{6}$$

Mathematically, this is associated with the ellipticity of the governing set of partial differential equations. Loss of ellipticity occurs if (6) holds. For plane strain isotropic linear elastic materials, following from (6), localisation of deformation does not occur if

$$G > 0 \quad \text{and} \quad -\infty < \nu < 0.5 \quad \text{or} \quad 1 < \nu < \infty. \tag{7}$$

Both (3) and (6) are local conditions, where (3) concerns uniform deformation and (6) localised deformation. From (4) and (7) it can been seen that for isotropic linear elasticity localisation of deformation (loss of ellipticity), for $0.5 < \nu < 1$, can only occur if there is loss of material stability (loss of positive-definiteness), for $\nu > 0.5$.

2.4 Uniqueness criterion by Cosserat for bounded domains

In the preceding local conditions of material stability and uniqueness were reviewed. Cosserat [12] was the first to consider bounded domains. The boundary value problem of homogeneous isotropic elasticity, consisting of the field equations of equilibrium and appropriate displacement boundary conditions as derived in detail in the following section by the authors, was investigated by Cosserat for particular domains. An analytical solution based on harmonic functions was assumed to derive the displacement field. As a sufficient condition for uniqueness of the solution in bounded domains the inequalities

$$G \neq 0 \quad \text{and} \quad -\infty < \nu < 0.5 \quad \text{or} \quad 1 < \nu < \infty, \tag{8}$$

were derived. Then, as a counter-example to uniqueness in the range $0.5 < \nu < 1.0$, Cosserat [12] showed for the circular domain, that a non-unique solution for the displacement boundary value problem of homogeneous isotropic elasticity exists for $\nu = 0.75$.

2.5 Well-posedness of the boundary value problem

In extension to the preceding, the (global) boundary value problem will be taken into consideration. A boundary value problem, consisting of a set of field equations and appropriate boundary conditions, is called well-posed if the problem has at least one solution (existence) and the problem has at most one solution (uniqueness) and the solution depends continuously on the input-data (mathematical stability).

In the case of a displacement boundary value problem, the implied conditions on the displacements on the boundary can restrain the existing sufficient local criteria for uniqueness and stability (Eqs. (1), (4) and (7)), leading to a stronger criterion, that will be necessary for the uniqueness of the solution of the global problem under consideration. Local discontinuities are constrained to propagate to the boundary. The uniqueness criterion as given in (7) has then to be reviewed. The question arises whether or not internal localisation can occur spontaneously in the particular range of Poisson's ratio between 0.5 and 1.0, while the displacements on the boundary still satisfy the implied conditions. For this reason consider a homogeneous (zero) implied boundary displacement. The homogeneous solution, i.e., zero displacements in the whole field, is always satisfying the boundary value problem. An internal localisation can occur if and only if a second displacement field coexists, that means only if the solution is non-unique. Therefore the problem involving the potential occurrence of internal localisation would be solved if a necessary condition for uniqueness could be established.

It should be noted that in the case of the traction boundary value problem local discontinuities can propagate to the boundary as no restrictions are imposed with respect to the displacements on the boundary. This case is not treated further in this paper.

For finite element meshes it is required that either no localised modes occur inside the finite elements (or if they could occur that they would be neglected). Consequently, a localisation would occur (or be allowed) at the scale of the elements, involving continuous deformation within the elements and along their boundaries. In such case the minimum thickness of the shear band would be described by the width of the element itself as a minimum. Therefore in the following the non-occurrence of element-internal instabilities will not be investigated as yet. Instead the analysis will focus on the well-posedness of the boundary value problem with continuous deformation within the elements and along their boundaries.

3 Formulation of the problem

The problem is formulated as a boundary value problem (BVP) in terms of displacements consisting of a system of partial differential equations (PDEs) and the appropriate number of boundary conditions. First, the system of PDEs is derived in tensor notation for a continuum before it is reduced to the plane strain situation and then elaborated in polar coordinates for the circular domain. Finally, the set of boundary conditions is stated to complete the BVP.

3.1 Definition of the basic equilibrium equations in a continuum

The system of PDEs is based on the field equation of linear elasticity for small strains. It can be derived by substituting Hooke's law for isotropic linear elastic material behaviour, $\boldsymbol{\sigma} = 2G[\boldsymbol{\varepsilon} + \nu/(1-2\nu)\boldsymbol{I}\,\mathrm{tr}(\boldsymbol{\varepsilon})]$, and the kinematic equation under the assumption of small displacements, $\boldsymbol{\varepsilon} = 1/2(\nabla \otimes \boldsymbol{u} + \boldsymbol{u} \otimes \nabla)$, into the equation of conservation of linear momentum in the static case assuming zero body force, $\nabla \boldsymbol{\cdot}\, \sigma = 0$. After some simplification it follows for $G \neq 0$,

$$2(1-\nu)\nabla(\nabla \boldsymbol{\cdot} \boldsymbol{u}) - (1-2\nu)\nabla \times (\nabla \times \boldsymbol{u}) = 0, \tag{9}$$

describing the equilibrium equation in a continuum in terms of displacements in the most general form without being coupled to any coordinate system. In the constitutive equations, $\boldsymbol{\sigma}$ is the Cauchy-stress tensor, $\boldsymbol{\varepsilon}$ the (small) linear strain tensor, $\boldsymbol{u}$ the displacement vector, and the constant material parameters: Poisson's ratio ν and shear modulus G. In tensor notation, $\otimes$ denotes the dyadic or outer tensor product, while $\boldsymbol{\cdot}$ denotes the dot or inner product of two tensors. $\boldsymbol{I}$ is the second order isotropic identity tensor, tr($\boldsymbol{\varepsilon}$) is the trace of the strain, and $\bigtriangledown$ the differential operator.

3.2 Derivation of the PDE for the plane strain situation

Consider now the general orthogonal curvilinear coordinates (ξ_1, ξ_2, ξ_3) in Euclidean 3-space with unit vectors $\{\boldsymbol{e}_1, \boldsymbol{e}_2, \boldsymbol{e}_3\}$. Each coordinate system can be characterised by metric coefficients g_{11}, g_{22}, g_{33}, defined as [24], [25]

$$g_{ii} = \left(\frac{\partial x_1}{\partial \xi_i}\right)^2 + \left(\frac{\partial x_2}{\partial \xi_i}\right)^2 + \left(\frac{\partial x_3}{\partial \xi_i}\right)^2, \quad (i = 1,2,3), \tag{10}$$

in which (x_1, x_2, x_3) are rectangular Cartesian coordinates. In the plane strain situation $\boldsymbol{u}$ is independent of the third coordinate direction ξ_3, and the displacements in this direction are fixed to be zero, i.e. $u_3 = 0$. A cylindrical coordinate system can be used for the description of the plane strain case. The first and second metric coefficient can be shown to be equal [23], $g_{11} = g_{22} = h^2$. They define the function $h(\xi_1, \xi_2) \neq 0$, depending on the first two coordinate directions only. The third metric coefficient is constant and reads $g_{33} = 1$. A set of coordinate system coefficients $H(\xi_1, \xi_2)$ can be defined as

$$H_{11} = \frac{1}{h}\left[\frac{\partial^2 h}{\partial \xi_1^2} - \frac{2}{h}\left(\frac{\partial h}{\partial \xi_1}\right)^2\right], \quad H_{22} = \frac{1}{h}\left[\frac{\partial^2 h}{\partial \xi_2^2} - \frac{2}{h}\left(\frac{\partial h}{\partial \xi_2}\right)^2\right],$$
$$H_{12} = \frac{1}{h}\left[\frac{\partial^2 h}{\partial \xi_1 \partial \xi_2} - \frac{2}{h}\frac{\partial h}{\partial \xi_1}\frac{\partial h}{\partial \xi_2}\right], \quad H_1 = \frac{1}{h}\frac{\partial h}{\partial \xi_1}, \quad H_2 = \frac{1}{h}\frac{\partial h}{\partial \xi_2}. \tag{11}$$

Using (11), the system of PDEs (9) can then be simplified for a general cylindrical coordinate system to

$$\left\{\begin{aligned}&2(1-v)\frac{\partial^2 u_1}{\partial\xi_1^2}+(1-2v)\frac{\partial^2 u_1}{\partial\xi_2^2}+2(1-v)H_{11}u_1+(1-2v)H_{22}u_1+\\&\quad+\frac{\partial^2 u_2}{\partial\xi_1\partial\xi_2}+H_{12}u_2+(3-4v)H_2\frac{\partial u_2}{\partial\xi_1}-(3-4v)H_1\frac{\partial u_2}{\partial\xi_2}\end{aligned}\right\}\boldsymbol{e}_1+$$
$$+\left\{\begin{aligned}&(1-2v)\frac{\partial^2 u_2}{\partial\xi_1^2}+2(1-v)\frac{\partial^2 u_2}{\partial\xi_2^2}+(1-2v)H_{11}u_2+2(1-v)H_{22}u_2+\\&\quad+\frac{\partial^2 u_1}{\partial\xi_1\partial\xi_2}+H_{12}u_1-(3-4v)H_2\frac{\partial u_1}{\partial\xi_1}+(3-4v)H_1\frac{\partial u_1}{\partial\xi_2}\end{aligned}\right\}\boldsymbol{e}_2=\mathbf{0}. \tag{12}$$

Note that the coordinate system coefficients $H(\xi_1,\ \xi_2)$ can be determined for each curvilinear, orthogonal, cylindrical coordinate system and are therefore known but variable coefficients, being functions of the coordinates $(\xi_1,\ \xi_2)$. For the circular cylinder system they will be elaborated in the next section.

For the classification of a system of PDEs only the second order derivatives are of importance. In system (12) it can be seen that the second order derivatives are not influenced by the choice of the cylindrical coordinate system as their preceding coefficients are constant with respect to the coordinate axes and depend only on the material parameter Poisson's ratio v and not on the coordinate system coefficients H. Therefore the transformation of the coordinate system and the domain to be studied is not changing the type of the PDE. However, it is not possible to give an exhaustive classification of the system of PDEs for this case as it is of a mixed type.

3.3 Reformulation of the PDE for the circular domain

In first instance a domain with a simple geometric configuration will be studied. That is the circle with its smooth boundary and its symmetrical properties. No problems with respect to corner points (e.g., discontinuities) will occur as for example in rectangular or triangular domains which are common in finite element calculations. Furthermore, for the circle only one single boundary condition at the outer boundary has to be applied without having to superpose different functions for each boundary edge.

For the circular domain and plane strain conditions the most suitable coordinate system is the circular-cylinder system with $\xi_1 = r\ (0 \le r \le R)$, $\xi_2 = \theta\ (0 \le \theta < 2\pi)$, and $\xi_3 = z$ $(-\infty < z < +\infty)$, in which r is the radius of the circle and θ the polar angle, see Fig. 1. The first and second metric coefficient are not equal anymore in this description, but they still define the auxiliary function $h = r$. Substitution of the preceding into (11) and the result into (12) gives the system of plane strain equilibrium equations for the circular domain as

$$\left\{\begin{aligned}&2(1-v)\frac{\partial^2 u_r}{\partial r^2}+(1-2v)\frac{1}{r^2}\frac{\partial^2 u_r}{\partial\theta^2}+2(1-v)\frac{1}{r}\frac{\partial u_r}{\partial r}-2(1-v)\frac{1}{r^2}u_r+\\&\quad+\frac{1}{r}\frac{\partial^2 u_\theta}{\partial r\partial\theta}-(3-4v)\frac{1}{r^2}\frac{\partial u_\theta}{\partial\theta}=0,\\&(1-2v)\frac{\partial^2 u_\theta}{\partial r^2}+2(1-v)\frac{1}{r^2}\frac{\partial^2 u_\theta}{\partial\theta^2}+(1-2v)\frac{1}{r}\frac{\partial u_\theta}{\partial r}-(1-2v)\frac{1}{r^2}u_\theta+\\&\quad+\frac{1}{r}\frac{\partial^2 u_r}{\partial r\partial\theta}+(3-4v)\frac{1}{r^2}\frac{\partial u_r}{\partial\theta}=0,\end{aligned}\right. \tag{13}$$

where u_r and u_θ are the radial and tangential displacements respectively, see Fig. 1.

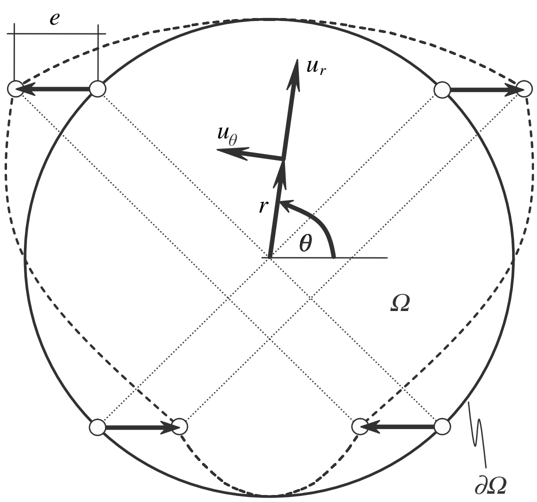

Fig. 1. Hourglass-like displacement boundary value problem in the circular domain Ω with boundary $\partial\Omega$ described by polar coordinates (r, θ); e is the magnitude of the prescribed nodal displacement

3.4 Definition of boundary conditions

To complete the boundary value problem a set of boundary conditions has to be defined for the 2-dimensional situation. For physical reasons the displacements and their derivatives with respect to r have to be bounded for all r and θ under consideration. Mathematically this is related to the assumption that the functions u_r and u_θ have to be twice continuously differentiable. Inside the circle Ω and on its boundary $\partial\Omega$ the displacements and their derivatives with respect to θ have to be periodic to guarantee continuity of displacements and strains,

$$\begin{aligned} u_r(r,0) &= u_r(r,2\pi), \quad \frac{\partial u_r(r,0)}{\partial\theta} = \frac{\partial u_r(r,2\pi)}{\partial\theta}, \\ u_\theta(r,0) &= u_\theta(r,2\pi), \quad \frac{\partial u_\theta(r,0)}{\partial\theta} = \frac{\partial u_\theta(r,2\pi)}{\partial\theta}. \end{aligned} \tag{14}$$

At the circle boundary $\partial\Omega$ the displacements in both the radial and tangential directions will be prescribed functions in θ:

$$u_r(r,\theta) = \varphi_r(\theta), \quad u_\theta(r,\theta) = \varphi_\theta(\theta). \tag{15}$$

Equations (13), (14) and (15) together with the assumption of boundedness form the complete boundary value problem, as illustrated in Fig. 1. In this figure the polar coordinate system (r, θ) as well as an example of the prescribed boundary conditions (15) are indicated. The displacement at the boundary is based on the magnitude of the nodal displacements e. The different possible deformation modes are indicated in Table 1.

4 Solution of the problem

Consider the general form of the equilibrium equations as given in (9). They are valid for $G \neq 0$. The solution is then independent of the shear modulus G. For $G = 0$ the set of equations has infinitely many solutions.

With respect to Poisson's ratio ν two special cases can be distinguished. The first case is related to $\nu = 0.5$. The field equations (9) simplify in tensor and index notation to $\nabla(\nabla \cdot \boldsymbol{u}) = 0$ or $u_{j,ij} = 0$, or elaborated for the circular domain

Table 1. Eight deformation modes of the circular domain with associated boundary conditions, calculated displacements and integrated strain energy, according to Rohe [30]

Deformation mode	Boundary condition φ (θ)	Displacements $u(\tilde{r}, \theta)$	Strain energy W
1-hor. translation	$\varphi_r = e\cos\theta$, $\varphi_\theta = -e\sin\theta$	$u_r = e\cos\theta$, $u_\theta = -e\sin\theta$	$W = 0$
2-vert. translation	$\varphi_r = e\sin\theta$, $\varphi_\theta = e\cos\theta$	$u_r = e\sin\theta$, $u_\theta = e\cos\theta$	$W = 0$
3-rotation	$\varphi_r = 0$, $\varphi_\theta = e$	$u_r = 0$, $u_\theta = e\tilde{r}$	$W = 0$
4-stretching	$\varphi_r = e\cos2\theta$, $\varphi_\theta = -e\sin2\theta$	$u_r = e\tilde{r}\cos 2\theta$, $u_\theta = -e\tilde{r}\sin 2\theta$	$W = 2\pi\ Ge^2/R$
5-shearing	$\varphi_r = e\sin2\theta$, $\varphi_\theta = e\cos2\theta$	$u_r = e\tilde{r}\sin 2\theta$, $u_\theta = e\tilde{r}\cos 2\theta$	$W = 2\pi\ Ge^2/R$
6-compression	$\varphi_r = -e$, $\varphi_\theta = 0$	$u_r = -e\tilde{r}$, $u_\theta = 0$	$W = \frac{2\pi Ge^2}{(1-2v)R}$
7-hor. hourglass	$\varphi_r = \frac{e}{2}(\sin\theta + \sin 3\theta)$ $\varphi_\theta = \frac{e}{2}(-\cos\theta + \cos 3\theta)$	$u_r = \left(\frac{1-4v}{3-4v}\tilde{r}^2 + \frac{2}{3-4v}\right)\frac{e}{2}\sin\theta + \frac{e}{2}\tilde{r}^2\sin 3\theta$ $u_\theta = -\left(\frac{5-4v}{3-4v}\tilde{r}^2 - \frac{2}{3-4v}\right)\frac{e}{2}\cos\theta + \frac{e}{2}\tilde{r}^2\cos 3\theta$	$W = \frac{4\pi(1-v)Ge^2}{(3-4v)R}$
8-vert. hourglass	$\varphi_r = \frac{e}{2}(\cos\theta - \cos 3\theta)$ $\varphi_\theta = \frac{e}{2}(\sin\theta + \sin 3\theta)$	$u_r = \left(\frac{1-4v}{3-4v}\tilde{r}^2 + \frac{2}{3-4v}\right)\frac{e}{2}\cos\theta - \frac{e}{2}\tilde{r}^2\cos 3\theta$ $u_\theta = \left(\frac{5-4v}{3-4v}\tilde{r}^2 - \frac{2}{3-4v}\right)\frac{e}{2}\sin\theta + \frac{e}{2}\tilde{r}^2\sin 3\theta$	$W = \frac{4\pi(1-v)Ge^2}{(3-4v)R}$

$$\begin{cases} r^2\dfrac{\partial^2 u_r}{\partial r^2} + r\dfrac{\partial u_r}{\partial r} - u_r + r\dfrac{\partial^2 u_\theta}{\partial r\partial\theta} - \dfrac{\partial u_\theta}{\partial\theta} = 0, \\ r\dfrac{\partial^2 u_r}{\partial r\partial\theta} + \dfrac{\partial u_r}{\partial\theta} + \dfrac{\partial^2 u_\theta}{\partial\theta^2} = 0. \end{cases} \tag{16}$$

The second case is related to $v = 1.0$. The field equations (9) simplify in tensor and index notation to $\nabla \times (\nabla \times \boldsymbol{u}) = 0$ or $u_{j,ij} - u_{i,jj} = 0$, or elaborated for the circular domain

$$\begin{cases} -\dfrac{\partial^2 u_r}{\partial\theta^2} + r\dfrac{\partial^2 u_\theta}{\partial r\partial\theta} + \dfrac{\partial u_\theta}{\partial\theta} = 0, \\ r\dfrac{\partial^2 u_r}{\partial r\partial\theta} - \dfrac{\partial u_r}{\partial\theta} - r^2\dfrac{\partial^2 u_\theta}{\partial r^2} - r\dfrac{\partial u_\theta}{\partial r} + u_\theta = 0. \end{cases} \tag{17}$$

To prove non-uniqueness it is sufficient to consider homogeneous boundary conditions $\boldsymbol{u} = \boldsymbol{0}$ on $\partial\Omega$, and to show that more than one solution exists in the field. Clearly, one solution is the homogenous solution, $\boldsymbol{u} = \boldsymbol{0}$ in Ω, as it satisfies the homogeneous boundary conditions and the field equations (16) and (17), respectively. For $v = 0.5$ a second solution is for example

$$\boldsymbol{u} = \begin{pmatrix} u_r \\ u_\theta \end{pmatrix} = \begin{pmatrix} 0 \\ r^2 - 1 \end{pmatrix}, \tag{18}$$

as it vanishes on the boundary for the unit circle and it satisfies the field equations (16). For $v = 1$ a second solution is for example

$$\boldsymbol{u} = \begin{pmatrix} u_r \\ u_\theta \end{pmatrix} = \begin{pmatrix} r^2 - 1 \\ 0 \end{pmatrix}, \tag{19}$$

as it vanishes on the boundary for the unit circle and it satisfies the field equations (17). Note that the solutions (18) and (19) can be found by trial and error, but are initiated by the work of Cosserat [12]. To summarise, for $G = 0$ or $v = 0.5$ or $v = 1.0$ the solution is non-unique as at least two solutions exist. The proof above can be converted and applied to other domains and the condition of non-uniqueness for $G = 0$, or for $v = 0.5$ or for $v = 1.0$ is valid for arbitrary domains.

4.1 Derivation of the general solution

In the following the solution for the case $G \neq 0$, and $\nu \neq 0.5$ and $\nu \neq 1.0$ will be derived. Consider the system of PDEs (13). It can be solved using an extended version of the method of separation of variables. A description can be found in [8], and an application can be found in [9], [26]. First, suppose a separated product form of the solution of (13) as

$$u_r(r,\theta) = f_r(r)\, g_r(\theta)\,, \quad u_\theta(r,\theta) = f_\theta(r)\, g_\theta(\theta), \tag{20}$$

where the functions f_r and f_θ depend only on the radius r, and the functions g_r and g_θ depend only on the polar angle θ. Substitution of (20) into the system of PDEs (13) leads after some rearrangement to a system of equations,

$$\begin{cases} \dfrac{2(1-\nu)}{1-2\nu}\left[\dfrac{r^2 f_r''}{f_r} + \dfrac{r f_r'}{f_r}\right] + \dfrac{1}{1-2\nu}\dfrac{g_\theta'}{g_r}\left[\dfrac{r f_\theta'}{f_r} - (3-4\nu)\dfrac{f_\theta}{f_r}\right] = -\dfrac{g_r''}{g_r} + \dfrac{2(1-\nu)}{1-2\nu}, & (21.1)\\[2ex] \dfrac{1-2\nu}{2(1-\nu)}\left[\dfrac{r^2 f_\theta''}{f_\theta} + \dfrac{r f_\theta'}{f_\theta}\right] + \dfrac{1}{2(1-\nu)}\dfrac{g_r'}{g_\theta}\left[\dfrac{r f_r'}{f_\theta} + (3-4\nu)\dfrac{f_r}{f_\theta}\right] = -\dfrac{g_\theta''}{g_\theta} + \dfrac{1-2\nu}{2(1-\nu)}, & (21.2) \end{cases}$$

in which the ordinary derivatives are defined as $f' = df/dr$, $f'' = d^2f/dr^2, g' = dg/d\theta$, and $g'' = d^2g/d\theta^2$. System (21) is generally supposed to be not separable due to the mixed terms. The extension of the method of separation of variables is based on the introduction of an additional differentiation step. Here, Eq. (21.1) is differentiated with respect to r. This equation then is reduced to the separable form,

$$-\frac{2(1-\nu)\frac{d}{dr}\left[\frac{r^2 f_r''}{f_r} + \frac{r f_r'}{f_r}\right]}{\frac{d}{dr}\left[\frac{r f_\theta'}{f_r} - (3-4\nu)\frac{f_\theta}{f_r}\right]} = \frac{g_\theta'}{g_r} = \mu\,, \quad \mu \in \mathbb{C}\,, \tag{22}$$

in which the complex valued separation constant μ is introduced. Equation (22) is separable as the left hand side depends only on r and the right hand side depends only on θ.

Substituting the right hand side of (22) into Eq. (21.2) for g_r' leads to the separable form

$$\frac{(1-2\nu)\left[\frac{r^2 f_\theta''}{f_\theta} + \frac{r f_\theta'}{f_\theta} - 1\right]}{2(1-\nu) + \frac{1}{\mu}\left[\frac{r f_r'}{f_\theta} + (3-4\nu)\frac{f_r}{f_\theta}\right]} = -\frac{g_\theta''}{g_\theta} = \eta\,, \quad \eta \in \mathbb{C}\,, \tag{23}$$

in which the complex valued separation constant η is introduced. The periodic boundary conditions (14) are used to solve the eigenvalue problem on the right hand side of (23). Solutions exist only for real eigenvalues $\eta = n^2$ with $n = 1, 2, 3, ...$, and are given by

$$g_\theta^{(n)}(\theta) = c_1^{(n)} \cos(n\theta) + c_2^{(n)} \sin(n\theta), \tag{24}$$

with so far undetermined coefficients $c_i^{(n)}$. Substituting the result (24) into the right hand side of (22) then gives, depending on the separation constant μ, the solutions for g_r for each $n = 1, 2, 3, ...$ as

$$g_r^{(n)}(\theta) = \frac{n}{\mu}\left[c_2^{(n)} \cos(n\theta) - c_1^{(n)} \sin(n\theta)\right]. \tag{25}$$

Substitution of the solutions (24) and (25) into the separated form of the system of PDEs (21) results in a 2-dimensional system of second order ordinary differential equations of the Euler-type for the functions f_r and f_θ, reading after some elaboration

$$\begin{cases} 2(1-v)\left[r^2 f_r'' + r f_r'\right] - \left[(1-2v)n^2 + 2(1-v)\right] f_r + \mu\left[r f_\theta' - (3-4v) f_\theta\right] = 0, \\ (1-2v)\left[r^2 f_\theta'' + r f_\theta'\right] - \left[2(1-v)n^2 + (1-2v)\right] f_\theta - \frac{n^2}{\mu}\left[r f_r' + (3-4v) f_r\right] = 0. \end{cases} \tag{26}$$

System (26) can be solved by looking for solutions for f_r and f_θ of the form

$$f_r = d_{i,1}^{(n)} r^{\lambda_i^{(n)}}, \quad f_\theta = d_{i,2}^{(n)} r^{\lambda_i^{(n)}}, \tag{27}$$

where $\lambda_i^{(n)} \in \mathbb{C}$ are eigenvalues, and where the constants $d_{i,1}^{(n)}$ and $d_{i,2}^{(n)}$ are components of the corresponding eigenvectors $\boldsymbol{d}_i^{(n)}$. Substituting the solutions (27) into (26), the characteristic system can be derived as

$$\begin{bmatrix} 2(1-v) & 0 \\ 0 & 1-2v \end{bmatrix} \begin{pmatrix} d_{i,1}^{(n)} \\ d_{i,2}^{(n)} \end{pmatrix} \left(\lambda_i^{(n)}\right)^2 + \begin{bmatrix} 0 & \mu \\ -n^2/\mu & 0 \end{bmatrix} \begin{pmatrix} d_{i,1}^{(n)} \\ d_{i,2}^{(n)} \end{pmatrix} \lambda_i^{(n)} + \\ - \begin{bmatrix} 2(1-v) + (1-2v)n^2 & (3-4v)\mu \\ (3-4v)n^2/\mu & (1-2v) + 2(1-v)n^2 \end{bmatrix} \begin{pmatrix} d_{i,1}^{(n)} \\ d_{i,2}^{(n)} \end{pmatrix} = \begin{pmatrix} 0 \\ 0 \end{pmatrix}. \tag{28}$$

Eigenvalues $\lambda_i^{(n)}$ and eigenvectors $\boldsymbol{d}_i^{(n)}$ can be determined by solving the characteristic equation of system (28). For the eigenvalues it follows, for $n = 0, 1, 2, \ldots$, that

$$\lambda_1^{(n)} = n+1, \quad \lambda_2^{(n)} = n-1, \quad \lambda_3^{(n)} = -n+1\,, \quad \lambda_4^{(n)} = -n-1. \tag{29}$$

Note that the eigenvalues are real and do not depend on the separation constant μ. For the eigenvectors it then follows for $n \neq 0$

$$\boldsymbol{d}_1^{(n)} = \begin{pmatrix} \omega^{(n)}\mu/n \\ 1 \end{pmatrix} \delta_1^{(n)}, \;\; \boldsymbol{d}_2^{(n)} = \begin{pmatrix} -\mu/n \\ 1 \end{pmatrix} \delta_2^{(n)}, \;\; \boldsymbol{d}_3^{(n)} = \begin{pmatrix} -\omega^{(n)}\mu/n \\ 1 \end{pmatrix} \delta_3^{(n)}, \;\; \boldsymbol{d}_4^{(n)} = \begin{pmatrix} \mu/n \\ 1 \end{pmatrix} \delta_4^{(n)}, \tag{30}$$

in which $\delta_i^{(n)}$ are remaining constants to satisfy the boundary conditions and an auxiliary constant,

$$\omega^{(n)} = \frac{2(1-2v) - n}{4(1-v) + n}. \tag{31}$$

Functions f_r and f_θ can now be composed by substituting (29) and (30) into the supposed general form of the solution (27). Then, by using the fact that the solutions should be bounded at the origin, the functions f_r and f_θ can be determined for each $n = 1, 2, 3, \ldots$ as

$$f_r^{(n)}(r) = \frac{\mu}{n}\left(\omega^{(n)} d_1^{(n)} r^2 - d_2^{(n)}\right) r^{n-1}\,, \tag{32}$$

$$f_\theta^{(n)}(r) = \left(d_1^{(n)} r^2 + d_2^{(n)}\right) r^{n-1}. \tag{33}$$

After substitution of (24), (25) and (32), (33) into the supposed separated product form of the solution (20), the general solution of the displacement field is determined as

$$\begin{cases} u_r(r,\theta) = \omega^{(0)} a_1^{(0)} r + \sum\limits_{n=1}^{\infty} r^{n-1}\left[\left(\omega^{(n)} a_1^{(n)} r^2 - a_2^{(n)}\right)\cos(n\theta) - \left(\omega^{(n)} b_1^{(n)} r^2 - b_2^{(n)}\right)\sin(n\theta)\right], \\ u_\theta(r,\theta) = b_1^{(0)} r + \sum\limits_{n=1}^{\infty} r^{n-1}\left[\left(b_1^{(n)} r^2 + b_2^{(n)}\right)\cos(n\theta) + \left(a_1^{(n)} r^2 + a_2^{(n)}\right)\sin(n\theta)\right]. \end{cases} \tag{34}$$

In (34), coefficients $a_i^{(n)}$, $b_i^{(n)}$ are combinations of the former coefficients $c_i^{(n)}$ and $d_i^{(n)}$. This solution satisfies the system of PDEs (13), the periodic boundary conditions (14), and the boundedness properties. It has the form of a full Fourier series in θ and is therefore complete. Also it should be noted that the separation constant μ does not occur in the general solution (34) for u_r as a result of the multiplicative combination of the solutions for f_r (25) and for g_r (32). When, instead of differentiating Eq. (21.1), Eq. (21.2) is differentiated with respect to r, the same results are obtained.

4.2 Application of general Dirichlet boundary conditions and uniqueness criterion

To determine the coefficients $a_1^{(0)}$ and $b_1^{(0)}$, and the coefficients $a_1^{(n)}$, $a_2^{(n)}$, $b_1^{(n)}$ and $b_2^{(n)}$ for $n = 1, 2, 3, \ldots$, occurring in the general solution (34) the two remaining boundary conditions for the prescribed displacements as given by (15) have to be used. Use is made of the orthogonality of the sine and cosine functions. To this end, first $r = R$ and the boundary conditions (15) are substituted into the general solution (34). Subsequently, the result is multiplied by cos $(m\theta)$ or sin $(m\theta)$ for $m = 0, 1, 2, \ldots$, respectively, and integrated with respect to θ on the whole domain $[0, 2\pi]$. For $m = 1, 2, 3, \ldots$ this leads to two linear systems of two equations, namely

$$\begin{cases} -R^{m-1}\left(\omega^{(m)} b_1^{(m)} R^2 - b_2^{(m)}\right) = \dfrac{1}{\pi}\displaystyle\int_0^{2\pi} \varphi_r(\theta)\sin(m\theta)d\theta = I_1^{(m)}, & m = 1,2,3,\ldots, \\ R^{m-1}\left(a_1^{(m)} R^2 + a_2^{(m)}\right) = \dfrac{1}{\pi}\displaystyle\int_0^{2\pi} \varphi_\theta(\theta)\sin(m\theta)d\theta = I_3^{(m)}, & m = 1,2,3,\ldots, \end{cases}$$
$$\begin{cases} R^{m-1}\left(\omega^{(m)} a_1^{(m)} R^2 - a_2^{(m)}\right) = \dfrac{1}{\pi}\displaystyle\int_0^{2\pi} \varphi_r(\theta)\cos(m\theta)d\theta = I_2^{(m)}, & m = 1,2,3,\ldots, \\ R^{m-1}\left(b_1^{(m)} R^2 + b_2^{(m)}\right) = \dfrac{1}{\pi}\displaystyle\int_0^{2\pi} \varphi_\theta(\theta)\cos(m\theta)d\theta = I_4^{(m)}, & m = 1,2,3,\ldots, \end{cases} \tag{35}$$

which defines also the constants $I_1^{(m)}$, $I_2^{(m)}$, $I_3^{(m)}$ and $I_4^{(m)}$ resulting from integration of the boundary conditions. For $m = 0$ it follows directly that,

$$a_1^{(0)} = \frac{1-\nu}{(1-2\nu)\pi R}\int_0^{2\pi} \varphi_r(\theta)d\theta\,, \quad b_1^{(0)} = \frac{1}{2\pi R}\int_0^{2\pi} \varphi_\theta(\theta)d\theta. \tag{36}$$

Then, for $m > 0$ the equations in (35) can be combined and rearranged for corresponding coefficients reading in matrix-vector notation as follows

$$\begin{bmatrix} R^2 & 1 \\ \omega^{(m)} R^2 & -1 \end{bmatrix} \begin{pmatrix} a_1^{(m)} \\ a_2^{(m)} \end{pmatrix} = R^{1-m} \begin{pmatrix} I_3^{(m)} \\ I_2^{(m)} \end{pmatrix}, \quad m = 1,2,3,\ldots,$$
$$\begin{bmatrix} R^2 & 1 \\ \omega^{(m)} R^2 & -1 \end{bmatrix} \begin{pmatrix} b_1^{(m)} \\ b_2^{(m)} \end{pmatrix} = R^{1-m} \begin{pmatrix} I_4^{(m)} \\ -I_1^{(m)} \end{pmatrix}, \quad m = 1,2,3,\ldots. \tag{37}$$

Both systems of linear equations in (37) are uniquely solvable if and only if the determinants of the matrices are non-zero. Non-unique solutions of (37) can exist if and only if the determinants are equal to zero. For both, the determinant reads

$$-\left(\omega^{(m)}+1\right)R^2=-\frac{2(3-4v)}{4(1-v)+m}R^2. \tag{38}$$

Therefore a unique solution exists for all $v \neq 0.75$. No solutions or non-unique solutions exist if and only if $v = 0.75$. Equation (38) is therefore called the necessary and sufficient criterion for uniqueness of the boundary value problem.

The unique part of the solution can then be determined by solving both systems in (37) for $v \neq 0.75$ and by calculating the coefficients. Substituting these coefficients into the general solution (34) results in

$$\begin{cases} u_r(\tilde{r},\theta)=\frac{1}{2}I_2^{(0)}\tilde{r}+\sum_{m=1}^{\infty}\frac{2(1-2v)-m}{2(3-4v)}\tilde{r}^{m-1}\Big\{\Big[(1-\tilde{r}^2)I_3^{(m)}+\Big(\tilde{r}^2+\frac{1}{\omega^{(m)}}\Big)I_2^{(m)}\Big]\cos(m\theta)+ \\ \qquad +\Big[(1-\tilde{r}^2)I_4^{(m)}+\Big(\tilde{r}^2+\frac{1}{\omega^{(m)}}\Big)I_1^{(m)}\Big]\sin(m\theta)\Big\}, \\ u_\theta(\tilde{r},\theta)=\frac{1}{2}I_4^{(0)}\tilde{r}+\sum_{m=1}^{\infty}\frac{4(1-v)+m}{2(3-4v)}\tilde{r}^{m-1}\Big\{\Big[(1-\tilde{r}^2)I_1^{(m)}+\Big(\tilde{r}^2+\omega^{(m)}\Big)I_4^{(m)}\Big]\cos(m\theta)+ \\ \qquad +\Big[(1-\tilde{r}^2)I_2^{(m)}+\Big(\tilde{r}^2+\omega^{(m)}\Big)I_3^{(m)}\Big]\sin(m\theta)\Big\}, \end{cases} \tag{39}$$

with constants $I_i^{(m)}$ as defined in (35), and the dimensionless radius $\tilde{r}=r/R$.

For $v = 0.75$, system (37) cannot be solved uniquely. The determinant of the matrix of (37) equals zero. Then either no solution or as in this case infinitely many solutions can exist. Substituting $v = 0.75$ into (37) gives the non-unique part of the solution as

$$\begin{cases} u_r(\tilde{r},\theta)=\frac{1}{2}I_2^{(0)}\tilde{r}+\sum_{m=1}^{\infty}\tilde{r}^{m-1}\Big[\Big(a_1^{(m)}R^{m+1}(1-\tilde{r}^2)+I_2^{(m)}\Big)\cos(m\theta)+ \\ \qquad +\Big(b_1^{(m)}R^{m+1}(\tilde{r}^2-1)+I_1^{(m)}\Big)\sin(m\theta)\Big], \\ u_\theta(\tilde{r},\theta)=\frac{1}{2}I_4^{(0)}\tilde{r}+\sum_{m=1}^{\infty}\tilde{r}^{m-1}\Big[\Big(b_1^{(m)}R^{m+1}(\tilde{r}^2-1)+I_1^{(m)}\Big)\cos(m\theta)+ \\ \qquad +\Big(a_1^{(m)}R^{m+1}(\tilde{r}^2-1)-I_2^{(m)}\Big)\sin(m\theta)\Big]. \end{cases} \tag{40}$$

The coefficients $a_1^{(m)}$ and $b_1^{(m)}$ remain undetermined in the solution and can take any real value. Note thus that solution (40) satisfies the system of PDEs (13), all the boundary conditions, (14) and (15), and the boundedness properties for $v = 0.75$.

5 Hourglass-like boundary conditions

For the prescribed displacements at the circle boundary $\partial\Omega$ (characterised by the functions φ_r and φ_θ as defined in (15)), eight different types of displacement modes can be distinguished, see Table 1 according to Rohe [27]. For the uniform deformation modes, i.e., 1 to 6, only unique solutions occur, as described for example in [4]. The ones leading to non-unique solutions are only the horizontal and vertical hourglass-like modes, 7 and 8. For the circle the prescribed boundary displacements in this case can be defined as

$$\begin{cases} \varphi_r(\theta)=e/2[\sin(\theta)+\sin(3\theta)], \\ \varphi_\theta(\theta)=e/2[-\cos(\theta)+\cos(3\theta)], \end{cases} \tag{41}$$

in which e is the magnitude of the prescribed enforced nodal displacement. See Fig. 1, in which an indication of the horizontal hourglass-like boundary condition is sketched.

Substituting the hourglass-like boundary conditions (41) into the right hand side of (35) to determine $I_i^{(m)}$ and this result into (39) gives for $v \neq 0.5,\ 0.75,\ 1$ the final solution for the dimensionless displacements in the circle as

$$\begin{cases} \dfrac{u_r(\tilde{r},\theta)}{e} = \left(\dfrac{1-4v}{2(3-4v)}\tilde{r}^2 + \dfrac{1}{3-4v}\right)\sin(\theta) + \dfrac{\tilde{r}^2}{2}\sin(3\theta)\,, \\ \dfrac{u_\theta(\tilde{r},\theta)}{e} = \left(\dfrac{4v-5}{2(3-4v)}\tilde{r}^2 + \dfrac{1}{3-4v}\right)\cos(\theta) + \dfrac{\tilde{r}^2}{2}\cos(3\theta). \end{cases} \tag{42}$$

For the other deformation modes the displacements are given in Table 1. From (42), the strain and stress fields can be determined as

$$\begin{cases} \varepsilon_{rr}\dfrac{R}{e} = \left[\dfrac{1-4v}{3-4v}\sin(\theta) + \sin(3\theta)\right]\tilde{r}, \\ \varepsilon_{\theta\theta}\dfrac{R}{e} = [\sin(\theta) - \sin(3\theta)]\tilde{r}, \\ \varepsilon_{r\theta}\dfrac{R}{e} = \left[-\dfrac{1}{3-4v}\cos(\theta) + \cos(3\theta)\right]\tilde{r}, \end{cases} \tag{43}$$

$$\begin{cases} \dfrac{\sigma_{rr}}{2G}\dfrac{R}{e} = \left[\dfrac{1}{3-4v}\sin(\theta) + \sin(3\theta)\right]\tilde{r}\,, \\ \dfrac{\sigma_{\theta\theta}}{2G}\dfrac{R}{e} = \left[\dfrac{3}{3-4v}\sin(\theta) - \sin(3\theta)\right]\tilde{r} \\ \dfrac{\sigma_{r\theta}}{2G}\dfrac{R}{e} = \left[-\dfrac{1}{3-4v}\cos(\theta) + \cos(3\theta)\right]\tilde{r}. \end{cases} \tag{44}$$

A visualisation of the displacement field is given in Fig. 2a for Poisson's ratio of $v = 0.45$. It can be observed that the solution along the boundary describes the hourglass-like conditions as imposed. The magnitude of the displacement in the nodes is one. At the bottom, top, left and right point of the circle boundary the displacement is zero. In the horizontal and vertical straight lines through the circle centre only vertical displacements occur. The maximum displacement occurs in the circle centre with a magnitude of $u/e = 0.83$. Shown in Fig. 2b is the plot of the principal stress field and in Fig. 2c the plot of the principal strain field for $v = 0.45$. For tensor fields, compression is denoted by a solid line, while tension is denoted by a dotted line. The principal stresses and strains are symmetric to the vertical axis and anti-symmetric to the horizontal axis. In the upper part of the circle mainly tensional stresses in horizontal direction occur with a maximum magnitude of $\sigma R/(2Ge) = 3.5$. The lower part is mainly subjected to horizontal compressional stresses with same magnitude. The maximum magnitude of principal strains is $\varepsilon R/e = 2$ as horizontal tension and vertical compression at the top. In the circle centre neither stresses nor strains occur.

6 Parametric study

Values of Poisson's ratio v between 0.5 and 1.0 can occur in equivalent linear elasticity when applied to dilatant granular materials, see for example Molenkamp [6]. This is also the range of special interest to study the stability of the solution, and therefore special attention is given to. The parametric study shown in Figs. 3 and 4 is carried out in a step-size of 0.15 for values of Poisson's ratio of 0.45, 0.60, 0.74, 0.76, 0.90 and 1.05. As for 0.75 no unique solution exists, two values close above (i.e. 0.76) and below (i.e. 0.74) are studied.

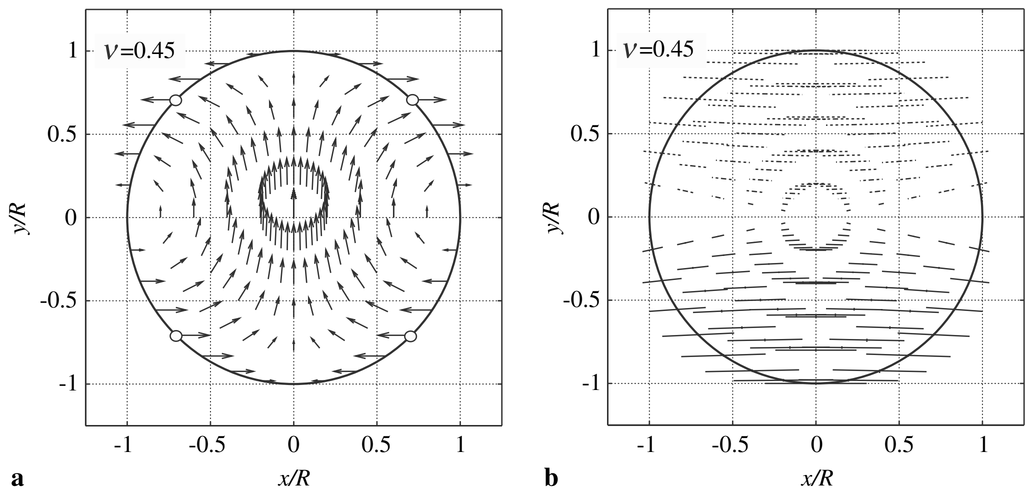

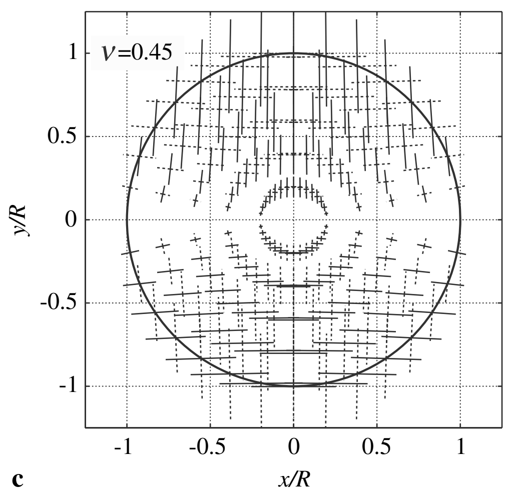

Fig. 2. Illustration of the solution for $\nu = 0.45$: **a** field of total displacements u/e; **b** principal stress tensor field $\sigma R/(2Ge)$; **c** principal strain tensor field $\varepsilon R/e$. Dotted lines denote tension, solid lines denote compression

In Fig. 3, the plot of the field of dimensionless total displacements u/e is given. Note that the scaling factor differs for the various values of ν for a clear visibility of the vectors. In the range $0.5 < \nu < 1.0$ the maximum displacement occurs at the circle centre while for values outside the maximum occurs at the nodes. Note the rigorous switch in direction of the displacements from $\nu = 0.74$ to $\nu = 0.76$. Whereas for $\nu = 0.74$ the displacement in the centre is directed vertically upwards with a magnitude of $u/e = 25$, at $\nu = 0.76$ the direction changes to vertically downwards with a magnitude of $u/e = 25$. This indicates the mathematical instability of the solution around the point $\nu = 0.75$. For a small change in the input parameter ν a large change in the result is observed. Along the boundary in all cases the implied hourglass-like boundary condition can be recognised.

In Fig. 4, the contour plots of the distribution of the total strain energy $W = 1/2(\sigma_{rr}\varepsilon_{rr} + \sigma_{\theta\theta}\varepsilon_{\theta\theta} + 2\sigma_{r\theta}\varepsilon_{r\theta})$, the strain energy due to isotropic deformation $W_{iso} = (1+\nu)/6(\varepsilon_{rr} + \varepsilon_{\theta\theta})(\sigma_{rr} + \sigma_{\theta\theta})$, and the strain energy due to deviatoric deformation, $W_{dev} = W - W_{iso}$, are given in the left, the middle, and the right column, respectively. The contour lines of the isotropic energy shown in the middle column of Fig. 4 run horizontally. The isotropic energy is directly related to the volumetric strain measure. At the horizontal centre-line it is always zero. The isotropic energy is

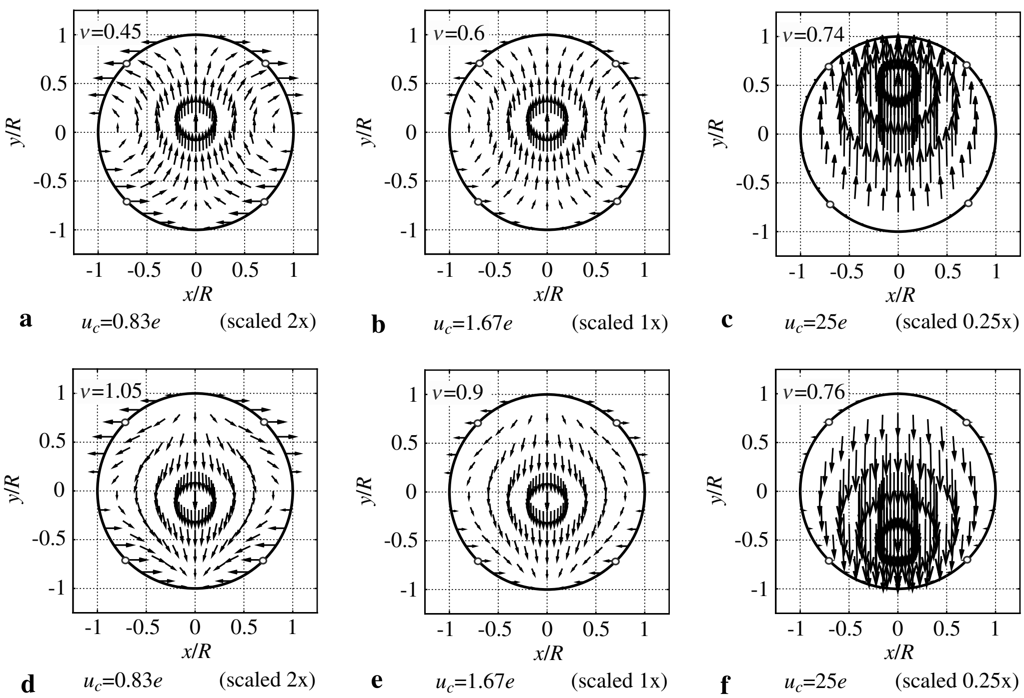

Fig. 3. Field of dimensionless total displacements u/e for $\nu = 0.45, 0.60, 0.74, 0.76, 0.90, 1.05$ plotted with different scaling factors. Magnitudes at the centre u_c are indicated

positive for $\nu < 0.50$, while for $\nu > 0.50$ it is negative in the whole field. For $\nu = 0.74$ and 0.76 the values at the top and bottom of the circle tend towards infinity, indicating the instability around this point. No switch in sign is observed around $\nu = 0.75$. The maximum and minimum values are always at the top and the bottom of the circle. The deviatoric energy shown in the right column of Fig. 4 is directly related to the deviatoric strain measure and remains positive for all values of ν in the whole field. Therefore the contour lines are almost horizontally distributed for $\nu < 0.5$. Reaching $\nu = 0.75$ these turn to be concentric circles. For $\nu > 0.75$ the distribution turns to be vertical. The maximum and minimum values are at the top and bottom of the circle for $\nu < 0.75$ and at the left and right for $\nu > 0.75$. In the centre the deviatoric energy is always zero. The total strain energy shown in the left column of Fig. 4 is the sum of both, the isotropic and deviatoric parts. For $\nu = 0.45$ the isotropic part is only a fraction of the deviatoric contribution. Around $\nu = 0.75$ the maximum absolute isotropic energy per unit of volume is several times larger than the corresponding maximum deviatoric energy while they are opposite in sign. Therefore the total energy does tend to infinity at $\nu = 0.75$, but less clear than the isotropic energy. The total energy is distributed horizontally for $\nu < 0.5$, turning to concentric horizontal ellipses at 0.6. For larger values the energy is distributed ''star-shaped'' with minimum (negative) values at the top and the bottom and maximum (positive) values at the left and the right. At the centre the total energy is zero.

To summarise the findings above, Fig. 5 shows the strain energy integrated over the whole domain versus Poisson's ratio ν to verify the behaviour of the solution around the points $\nu = 0.5, 0.75, 1.0$. The total strain energy W_{tot} is contributed by the isotropic part W_{iso} and the deviatoric part W_{dev}. Around $\nu = 0.75$ all three values tend asymptotically to infinity, indicating the mathematical instability around this point. At $\nu = 0.5$ and 1.0 the limits from above and below these magnitudes of Poisson's ratio ν reach the same value of the total strain energy. The solution is continuous there,

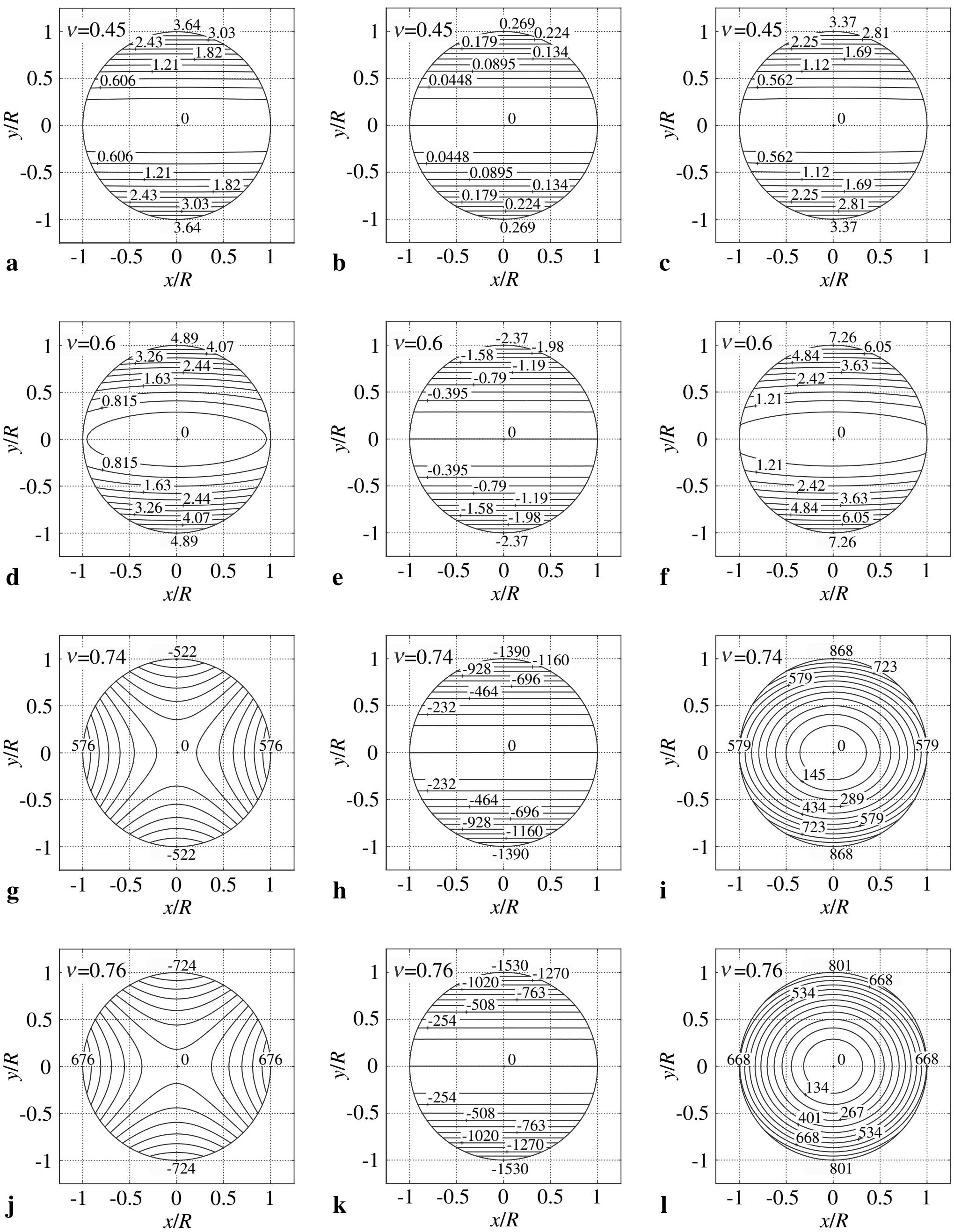

Fig. 4. Total (*left*), isotropic (*middle*) and deviatoric (*right*) strain energy distribution for $\nu = 0.45$, 0.60, 0.74, 0.76, 0.90, 1.05

indicating the mathematical stability around this point. The deviatoric energy is positive in the whole domain, whereas the isotropic energy is positive only for $\nu < 0.5$. For all deformation modes the analytic expressions of the integrated strain energy in the circle are given in Table 1. The expressions are comparable to the eigenvalues of the element stiffness matrix found by Molenkamp [6] for the isoparametric four-node isotropic linear elastic square element.

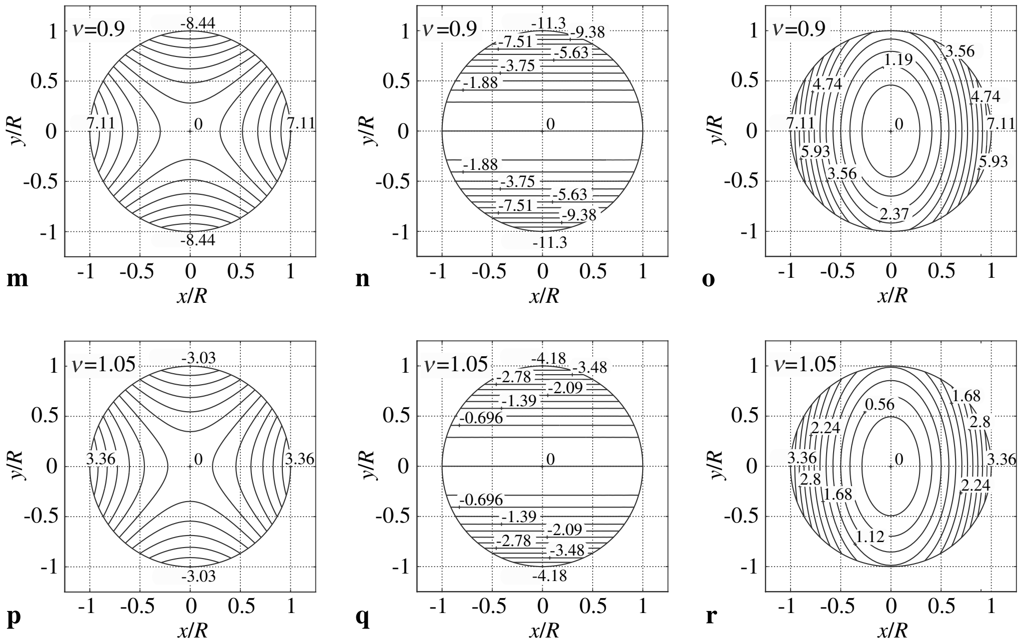

Fig. 4 (Continued). Total (*left*), isotropic (*middle*) and deviatoric (*right*) strain energy distribution for $\nu = 0.45, 0.60, 0.74, 0.76, 0.90, 1.05$

7 Evaluation

Comparison of the results above with the results for the square shaped area, Molenkamp [6], demonstrates that the removal of the corners by changing from a square to a circle increases the Poisson's ratio ν range with positive total energy from about $\nu < 0.6$ to $\nu < 0.75$. Like for the square also for the circle at this limit 'locking' occurs due to infinite total energy occurring as illustrated in Fig. 5. For the polar angles $\theta = 0$ and $\theta = \pi/2$ the local strain energy per unit of area along the circular boundary approaches $+\infty$ and $-\infty$ respectively for $\nu \uparrow 0.75$.

In the next phase of the ongoing research the system of partial differential equations will also be elaborated for Mohr-Coulomb elasto-plasticity including hardening. This material model is widely used in geotechnical engineering to describe soil behaviour and was used in the unexplained problems [1]–[3] under investigation. This material model also includes elasto-plastic dilation and a non-associative flow rule. It is expected that a further extension of the method will also supply closed form analytical solutions and necessary and sufficient uniqueness criteria for different kinds of elements, like elliptical (artificial) and rectangular ones. For triangular elements the solution is expected to be possible as the displacement field will be uniform.

8 Conclusion

The boundary value problem of linear elastostatics has been derived in terms of displacements for arbitrary domains. Then for the circular domain, with hourglass-like boundary conditions the closed form analytical solution has been derived using an extended version of the method of separation of variables. It has been shown that there exists at least one solution for all $G \in \mathbb{R}$ and all $\nu \in \mathbb{R}$. At most one solution exists for all $G \neq 0$ and all $\nu \neq 0.5, 0.75, 1$. The solution is mathematically stable

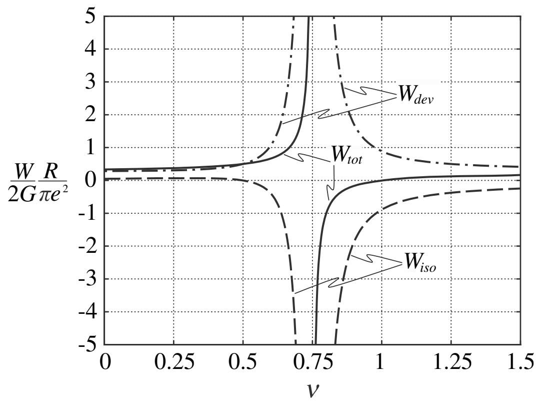

Fig. 5. Integrated strain energy W_{tot} as a function of ν, split up into deviatoric part W_{dev} and isotropic part W_{iso}

Table 2. Summary of the mathematical stability and uniqueness of the hourglass-like Dirichlet boundary value problem for the circular interior domain

parameter G	parameter ν	Mathematical stability	uniqueness
$G = 0$	$\nu \in \mathbb{R}$	–	no
$G \neq 0$	$\nu = 0.5$	yes	no
	$\nu = 0.75$	no	no
	$\nu = 1$	yes	no
	$\nu \neq 0.5, 0.75, 1.0$	yes	yes

for all $G \neq 0$ and all $\nu \neq 0.75$. Combined this means that the problem is well-posed for the shear modulus $G \neq 0$ and for all values of Poisson's ratio $\nu \neq 0.5, 0.75, 1$. The results are summarised in Table 2. At $\nu = 0.75$ for the circle in the case of plane strain linear isotropic elasticity locking of the element occurs due to the fact that the total strain energy becomes infinite. The local strain energy per unit of area along the circular boundary approaches $+\infty$ and $-\infty$ for $\nu \uparrow 0.75$ and $\nu \downarrow 0.75$, respectively.

The character of the system of partial differential equations is not changed by the choice of the coordinate system or domain. That means that non-unique solutions will stay to occur at the points $G = 0$ and $\nu = 0.5, 1$ also for the rectangular or arbitrary domain. However, the choice of the boundary may influence the nature of the remaining non-unique parameter range.

References

[1] Vermeer, P. A., Van Langen, H.: Soil collapse computations with finite elements. Ing. Arch. **59**, 221–236 (1989).

[2] De Borst, R., Vermeer, P. A.: Possibilities and limitations of finite elements for limit analysis. Géotechnique **34**, 199–210 (1984).

[3] Van der Veen, H. I.: The significance and use of eigenvalues and eigenvectors in the numerical analysis of elasto-plastic soils. Ph.D.-Thesis, Delft University of Technology (1998).

[4] Sellmeijer, J. B.: Stability of finite element: hour-glassing deformation. Report of GeoDelft, SE-, 703452 (1991).

[5] Lewis, E. B.: An analytical and numerical study of plane finite elements. Ph.D.-Thesis, University of Manchester, Institute of Science and Technology (1995).

[6] Molenkamp, F., Sellmeijer, J. B., Sharma, C. B., Lewis, E. B.: Explanation of locking of four-node plane element by considering it as elastic Dirichlet-type boundary value problem. Int. J. Numer. Anal. Meth. Geomech. **24**, 1013–1048 (2000).

[7] Molenkamp, F., Lewis, E. B., Sharma, C. B., Sellmeijer, J. B.: Fractal approach applied to calculate hour-glass eigenvalue of elastic square 4-node quad. Int. J. Numer. Anal. Meth. Geomech. **24**, 1049–1060 (2000).

[8] van Horssen, W. T.: On the applicability of the method of separation of variables for partial difference equations. J. Diff. Eq. Appl. **8**, 53–60 (2002).

[9] van Horssen, W. T., Zarubinskaya, M. A.: On an elastic dissipation model for a cantilevered beam. Q. J. Appl. Math. **61**, 565–573 (2003).

[10] Kirchhoff, G.: Über das Gleichgewicht und die Bewegung einer elastischen Scheibe. J. Reine Angew. Math. **40**, 51–88 (1850).

[11] Kirchhoff, G.: Über das Gleichgewicht und die Bewegung eines unendlich dünnen elastischen Stabes. J. Reine Angew. Math. **56**, 285–313 (1859).

[12] Cosserat E., Cosserat F.: Sur les équations de la théorie de l'élasticité. C.R. Acad. Sci. Paris **126**, 1089–1091 (1898); Sur les fonctions potentielles de la théorie de l'élasticitè. C.R. Acad. Sci. Paris **126**, 1129–1132 (1898); Sur la déformation infiniment petite d'un ellipsoïde élastique. C.R. Acad. Sci. Paris **127**, 315–318 (1898); Sur la solution des équations de l'élasticitè, dans le cas où les valeurs des inconnues à la frontière sont données. C.R. Acad. Sci. Paris **133**, 145–147 (1901); Sur la déformation infiniment petite d'un corps élastique soumis à des forces données. C.R. Acad. Sci. Paris **133**, 271–273 (1901); Sur la déformation infiniment petite d'une enveloppe sphérique élastique. C.R. Acad. Sci. Paris **133**, 326–329 (1901); Sur la déformation infiniment petite d'un ellipsoïde élastique soumis à des efforts donnés sur la frontière. C.R. Acad. Sci. Paris **133**, 361–364 (1901).

[13] Ericksen, J. L.: On the Dirichlet problem for linear differential equations. Proc. Am. Math. Soc. **8**, 521–522 (1957).

[14] Ericksen, J. L.: Non-existence theorems in linear elasticity theory. Arch. Rat. Mech. Anal. **14**, 180–183 (1963).

[15] Gurtin, M. E., Sternberg, E.: On the first boundary-value problem of linear elastostatics. Arch. Rat. Mech. Anal. **6**, 177–187 (1960).

[16] Bramble, J. H., Payne, L. E.: Some uniqueness theorems in the theory of elasticity. Arch. Rat. Mech. Anal. **9**, 319–328 (1962).

[17] Hill, R.: On uniqueness and stability in the theory of finite elastic strain. J. Mech. Phys. Solids **5**, 229–241 (1957).

[18] Hill, R.: A general theory of uniqueness and stability in elastic-plastic solids. J. Mech. Phys. Solids **6**, 236–249 (1958).

[19] Hill, R.: Uniqueness in general boundary-value problems for elastic or inelastic solids. J. Mech. Phys. Solids **9**, 114–130 (1961).

[20] Zervos, A., Papanastasiou, P., Vardoulakis, I.: Modelling of localisation and scale effect in thick-walled cylinders with gradient elastoplasticity. Int. J. Solid Struct. **38**(30–31), 5081–5095 (2001).

[21] Chambon, R., Caillerie, D.: Existence and uniqueness theorems for boundary value problems involving incrementally nonlinear models. Int. J. Solid Struct. **36**(33), 5089–5099 (1999).

[22] Rudnicki, J. W., Rice, J. R.: Conditions for the localization of deformation in pressure sensitive dilatant materials. J. Mech. Phys. Solids **23**, 371–394 (1975).

[23] Landau, L. D., Lifshitz, E. M.: Theory of elasticity. Oxford: Pergamom 1959.

[24] Morse, P. M., Feshbach, H.: Methods of theoretical physics. New York: McGraw-Hill 1953.

[25] Moon, P., Spencer, D. E.: Field theory handbook. Including coordinate systems, differential equations and their solutions, 2nd ed. Berlin: Springer 1971.

[26] Rohe, A., Molenkamp, F., van Horssen, W. T.: Investigation of material parameter field at the limits of existence and uniqueness of finite elements for applications in geomechanics. In: Prediction, analysis and design in geomechanical applications (Barla, G., Barla, M., eds.), pp. 159–166, 11th Int. Conf. of IACMAG, Turin, Italy 2005. Bologna: Pàtron editore 2005.

[27] Rohe, A., Molenkamp, F., van Horssen, W. T.: Uniqueness and stability of plane boundary value problems in finite element description. In: 10th Int. Symp. on Numerical Models in Geomechanics, Rhodes, Greece 2007.